Narrow linewidth picosecond UV pulsed laser with mega-watt peak power

Chunning Huang, Craig Deibele, and Yun Liu*

Spallation Neutron Source, Oak Ridge National Laboratory, 1 Bethel Valley Road, Oak Ridge, TN 37831, USA
*liuy2@ornl.gov

Abstract: We demonstrate a master oscillator power amplifier (MOPA) burst mode laser system that generates 66 ps/402.5 MHz pulses with mega-watt peak power at 355 nm. The seed laser consists of a single frequency fiber laser (linewidth < 5 KHz), a high bandwidth electro-optic modulator (EOM), a picosecond pulse generator, and a fiber based preamplifier. A very high extinction ratio (45 dB) has been achieved by using an adaptive bias control of the EOM. The multi-stage Nd:YAG amplifier system allows a uniformly temporal shaping of the macropulse with a tunable pulse duration. The light output from the amplifier is converted to 355 nm, and over 1 MW peak power is obtained when the laser is operating in a 5-μs/10-Hz macropulse mode. The laser output has a transform-limited spectrum with a very narrow linewidth of individual longitudinal modes. The immediate application of the laser system is the laser-assisted hydrogen ion beam stripping for the Spallation Neutron Source (SNS).

OCIS codes: (140.0140) Lasers and laser optics; (140.3538) Lasers, pulsed; (140.3610) Lasers, ultraviolet.

References and links

1. I. Will, G. Koss, and I. Templin, "The upgraded photocathode laser of the TESLA Test Facility," Nucl. Instrum. Methods Phys. Res. A **541**(3), 467–477 (2005).
2. S. Zhang, D. Hardy, G. Neil, and M. Shinn, "Characterization and performance of a high-power solid-state laser for a high-current photo-cathode injector," in *Proc. 27th International Free Electron Laser Conference* (SLAC, 2005), pp. 351–354.
3. K. Sakaue, M. Washio, S. Araki, M. Fukuda, Y. Higashi, Y. Honda, T. Omori, T. Taniguchi, N. Terunuma, J. Urakawa, and N. Sasao, "Observation of pulsed x-ray trains produced by laser-electron Compton scatterings," Rev. Sci. Instrum. **80**(12), 123304 (2009).
4. V. Danilov, A. Aleksandrov, S. Assadi, J. Barhen, W. Blokland, Y. Braiman, D. Brown, C. Deibele, W. Grice, S. Henderson, J. Holmes, Y. Liu, A. Shishlo, A. Webster, and I. N. Nesterenko, "Proof-of-principle demonstration of high efficiency laser-assisted H^- beam conversion to protons," Phys. Rev. ST Accel. Beams **10**(5), 053501 (2007).
5. R. Knappe, H. Haloui, A. Seifert, A. Weis, and A. Nebel, "Scaling ablation rates for picosecond lasers using burst micromachining," Proc. SPIE **7585**, 75850H (2010).
6. J. D. Fowlkes, L. Kondic, J. Diez, Y. Wu, and P. D. Rack, "Self-assembly versus directed assembly of nanoparticles via pulsed laser induced dewetting of patterned metal films," Nano Lett. **11**(6), 2478–2485 (2011).
7. A. Agnesi, C. Braggio, L. Carrà, F. Pirzio, S. Lodo, G. Messineo, D. Scarpa, A. Tomaselli, G. Reali, and C. Vacchi, "Laser system generating 250-mJ bunches of 5-GHz repetition rate, 12-ps pulses," Opt. Express **16**(20), 15811–15815 (2008).
8. Y. Liu, "Advancements in laser technology and applications to accelerators," presented at the Proc. HB2010, Morschach, Switzerland, TUO2B04–1-4 (2010).
9. A. Malinowski, K. T. Vu, K. K. Chen, J. Nilsson, Y. Jeong, S. Alam, D. Lin, and D. J. Richardson, "High power pulsed fiber MOPA system incorporating electro-optic modulator based adaptive pulse shaping," Opt. Express **17**(23), 20927–20937 (2009).
10. L. Lago, A. Mussot, M. Douay, and E. Hugonnot, "Single-mode narrow-bandwidth temporally shaped nanosecond-pulse ytterbium-doped fiber MOPA for a large-scale laser facility front-end," J. Opt. Soc. Am. B **27**(11), 2231–2236 (2010).
11. A. Agnesi, L. Carrà, P. Dallocchio, F. Pirzio, G. Reali, S. Lodo, and G. Piccinno, "50-mJ macro-pulses at 1064 nm from a diode-pumped picosecond laser system," Opt. Express **19**(21), 20316–20321 (2011).
12. H. Kalaycıoğlu, Y. B. Eldeniz, Ö. Akçaalan, S. Yavaş, K. Gürel, M. Efe, and F. Ö. Ilday, "1 mJ pulse bursts from a Yb-doped fiber amplifier," Opt. Lett. **37**(13), 2586–2588 (2012).

#183038 - $15.00 USD Received 8 Jan 2013; revised 25 Mar 2013; accepted 28 Mar 2013; published 4 Apr 2013

13. J. Kondo, K. Aoki, A. Kondo, T. Ejiri, Y. Iwata, A. Hamajima, T. Mori, Y. Mizuno, M. Imaeda, Y. Kozuka, O. Mitomi, and M. Minakata, "High-speed and low-driving-voltage thin-sheet x-cut $LiNbO_3$ modulator with laminated low-dielectric-constant adhesive," IEEE Photon. Technol. Lett. **17**(10), 2077–2079 (2005).
14. T. Sakamoto, T. Kawanishi, and M. Tsuchiya, "10 GHz, 2.4 ps pulse generation using a single-stage dual-drive Mach-Zehnder modulator," Opt. Lett. **33**(8), 890–892 (2008).
15. D. von der Linde, "Characterization of the noise in continuously operating mode-locked lasers," Appl. Phys. B **39**(4), 201–217 (1986).
16. P. Horak and W. H. Loh, "On the delayed self-heterodyne interferometric technique for determining the linewidth of fiber lasers," Opt. Express **14**(9), 3923–3928 (2006).
17. B. Moslehi, "Noise power spectra of optical two-beam interferometers induced by the laser phase noise," J. Lightwave Technol. **4**(11), 1704–1710 (1986).
18. T. Habruseva, S. O'Donoghue, N. Rebrova, F. Kéfélian, S. P. Hegarty, and G. Huyet, "Optical linewidth of a passively mode-locked semiconductor laser," Opt. Lett. **34**(21), 3307–3309 (2009).
19. Y. Liu, C. Huang, and A. Aleksandrov, "Laser optics development for the laser-assisted H- beam stripping at Spallation Neutron Source," in *IEEE Proceedings on IQEC/CLEO Pacific Rim 2011*, (IEEE, 2011), pp. 881–883 (2011).

1. Introduction

An increasing number of laser applications require lasers operating in a macropulsed or burst mode where each macropulse contains many micropulses at high repetition rates and narrow pulse widths although the macropulse itself is repeated at a much lower repetition rate. In laser-particle interaction systems such as photo injectors [1,2], Compton scattering based X-ray/γ-ray generators [3], and very recently laser-assisted ion beam stripping experiments [4], the macropulses are typically running at a few Hz to a few tens of Hz to fit the accelerator baseline, while the micropulses are normally required to have ~100 MHz repetition rates and picosecond pulse widths to match the micro-bunch of the particle beam. The macropulse mode of operation has also been found to be useful in ultrafast material processing [5], laser-induced nano droplet dewetting [6], as well as quantum physics research [7]. In many of the above applications, in particular photo-particle interactions, a mega-watt peak power at UV wavelength is often needed [8].

To produce sufficient peak power and offer flexibility of pulse parameters, almost all of the macropulse mode laser systems involve a master oscillator power amplifier (MOPA) configuration. The majority of the master oscillators, or the seeders, uses actively or passively mode-locked lasers based on semiconductor or fiber-optic technologies to generate picosecond optical pulse trains at a high repetition rates [1–3,7–12]. In these technologies, however, the laser cavity should be designed and stabilized to generate stable pulse trains, which reduces flexibility in the operation. Especially in the case of many actively mode-locked fiber lasers operating at high repetition frequencies, the cavity length is locked to a sub-harmonic of the repetition frequency. This scheme often induces mode hopping and side mode noise in its operation. Moreover, there is very limited tuneability in its pulse width. On the other hand, owing to the improvement in modulation bandwidth and the decrease in driving voltage, short pulse generation using electro-optic (EO) modulators has recently been attracting renewed attention [13,14].

In this paper, we demonstrate a narrow linewidth, mode-hopping free picosecond pulsed laser system in the MOPA configuration by using an electro-optic modulator (EOM) based pulse generation. The high contrast (> 40 dB), picosecond pulses are achieved by directly modulating a single-frequency fiber laser output with 402.5 MHz/80 ps RF pulses using an ultra-high extinction ratio EOM with adaptive bias control. A Yb-doped fiber amplifier (YDFA), multi-stage Nd:YAG amplifiers, pulse picker, waveform shaping algorithm and harmonic conversion crystals are employed to achieve a high repetition rate, macropulsed UV light source. The laser system is developed for the laser-assisted hydrogen ion (H^-) beam stripping experiment conducted at the Spallation Neutron Source (SNS) [15]. While the laser parameters demonstrated in the present work are intended to match the SNS H^- beam specifications, e.g. ~50 ps pulse width at 402.5 MHz repetition rate, the laser system has a broad parameter flexibility and the design concept can be useful in many other applications [1–7].

#183038 - $15.00 USD Received 8 Jan 2013; revised 25 Mar 2013; accepted 28 Mar 2013; published 4 Apr 2013

2. Experimental setup

Figure 1 shows a schematic of the laser system. The laser system contains a master oscillator, multi-stage Nd:YAG amplifiers, and harmonic converters. The master oscillator consists of a CW fiber laser, a Mach-Zehnder (MZ) intensity electro-optical modulator (EOM), and a ytterbium-doped fiber amplifier (YDFA). The fiber laser has a 50 mW single frequency light output around 1064.5 nm with a very narrow linewidth (<5 KHz) and the wavelength is tunable over 0.15 nm. The laser output is modulated by an EOSPACE 20 Gpbs $LiNbO_3$ EOM with ~80 ps, 402.5 MHz pulses produced from a customized radio-frequency (RF) pulse generator. The EOM output is then pre-amplified by a polarization-maintaining (PM) YDFA (Amonics YDFA-B) that provides a gain of 30 dB with an average output power of up to 200 mW.

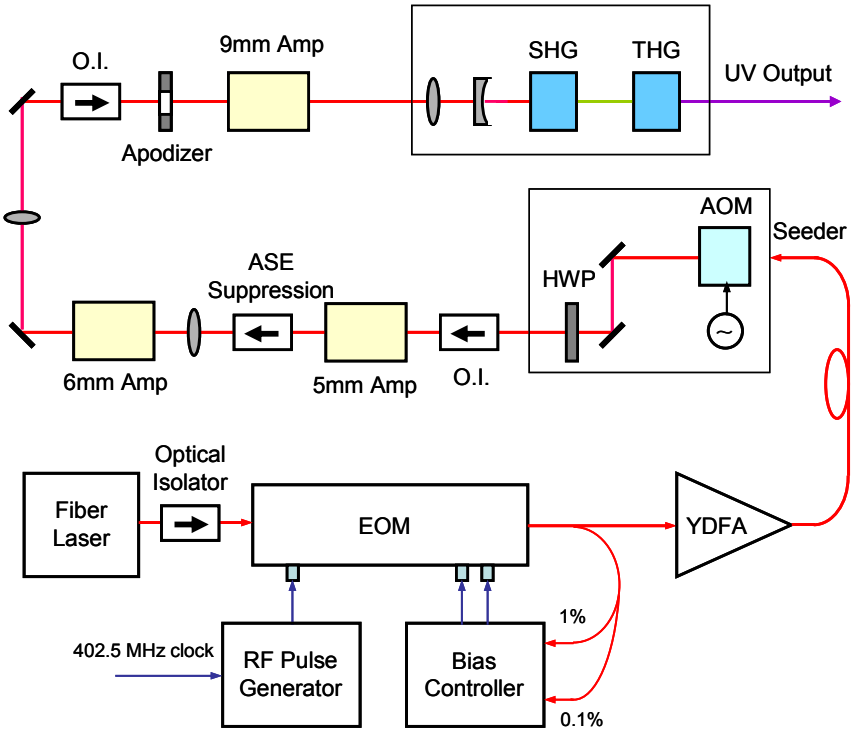

Fig. 1. Schematic of laser system: EOM, electro-optic modulator; RF, radio frequency; YDFA, Yb-doped fiber amplifiers; AOM, acousto-optic modulator; HWP, half-wave plate; O.I., optical isolator; ASE, amplified spontaneous emission; SHG (THG): second (third) harmonic generator.

Prior to the Nd:YAG amplifiers, the output light from the YDFA is injected into an acousto-optic modulator (AOM) through a PM fiber for macropulse generation and shaping. Unlike in the previous work [9,10] where the pulse generation and shaping were conducted using an EOM or a combination of AOM and EOM, here both are done using a single AOM. A voltage-controlled RF amplifier drives the AOM at a fixed frequency close to the AOM resonance (41 MHz). The macropulse shape is controlled with a wave shaper program through a Stanford DS345 synthesized-function generator that converts the waveform generated on a Continuum graphical user interface (GUI) into a voltage signal with a variable amplitude and applies it to the voltage-controlled RF amplifier. The amplitude of the RF signal determines the amount of seed light directed into the amplification chain. The maximum diffraction efficiency of the 1st order beam of the AOM is measured to be about 80%. Through controlling the RF pulse profile, one can achieve an arbitrary pulse shape out of the end of the amplifiers. The main purpose of having the shaping capability is to combat

#183038 - $15.00 USD Received 8 Jan 2013; revised 25 Mar 2013; accepted 28 Mar 2013; published 4 Apr 2013

the effects of gain saturation in the amplifier chain. The pulse being amplified is short compared to the lamp pulse. Therefore, the first part of the pulse envelope sees the highest gain and this gain is depleted as the pulse envelope passes through the rods. To achieve a flat macropulse of the UV light, the macropulse of the seed light is controlled so that the front end of the pulse envelope has less energy than the end of the pulse envelope, thus compensating for this gain depletion. A typical GUI generated control waveform for a 5 μs macro-pulse is shown in Fig. 2. The repetition frequency of the macro pulse is limited by the saturation of the amplifiers. At the current experiment, the macro pulse is repeating at 10 Hz. The actual driving signal of the AOM consists of 41 MHz RF oscillations whose amplitude is modulated by the waveform in Fig. 2.

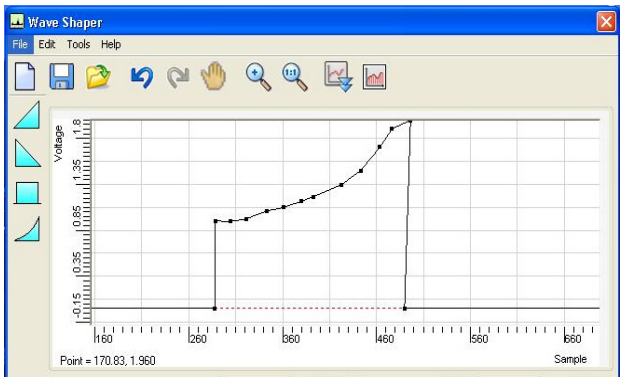

Fig. 2. Control waveform generated in GUI for 5 μs macro-pulse.

An additional feature of the AOM is to maintain high polarization extinction ratio through polarization switch. The diffracted beam from the AOM changes its polarization from horizontal to vertical and the optics are designed so that only the vertically polarized light is sent to the amplifiers. Two stages of Faraday isolators are installed between the AOM and amplifiers to protect the seeder from any optical feedback from the rest of the laser amplifier chain.

The Continuum customized macropulse amplifier system contains three amplification stages of 5 mm, 6 mm, and 9 mm Nd:YAG heads, respectively. Each amplification stage consists of two YAG rods and two pieces of optics between the rods: a negative lens for compensation of thermal lensing in the heads and a quartz rotator for compensation of the thermal birefringence from the heads. A Pockels cell is installed after the 5 mm amplification stage and the delay time between the Pockels trigger and the flash lamp is properly adjusted to prevent the laser from generating too much forward-propagating amplified spontaneous emission (ASE) that will rob the gain from the main pulse. A Faraday isolator is installed after the 6 mm amplification stage to eliminate light reflection. Relay imaging lenses and spatial filter pinholes are installed between amplification stages to control the beam profile. Finally, a ϕ5-mm apodizer is installed before the 9 mm amplification stage to optimize the spatial profile of the laser output.

At the end of the laser system, the wavelength conversion part contains a pair of lenses for beam collimation, a 25 mm long LBO crystal for the second harmonic generation, and a 30 mm long LBO crystal for the third harmonic generation. The 1064/532/355 wavelengths are separated by a couple of dichroic mirrors. Due to the space limitation, no dispersion compensation optics are used between the doubler and the tripler. The group velocity mismatch coming from the harmonic generation crystals is estimated to cause a few picoseconds of pulse broadening which is acceptable for our application.

#183038 - $15.00 USD Received 8 Jan 2013; revised 25 Mar 2013; accepted 28 Mar 2013; published 4 Apr 2013

3. Experimental results

3.1 Seeder performance

Stable frequency, narrow linewidth, low timing jitter and high extinction ratio are critical parameters for the seed light. The wavelength of the fiber laser is stabilized at 1064.45 nm to maximize the gain of the Nd:YAG amplifiers. The linewidth of the fiber laser is less than 5 KHz. The fiber laser output is coupled to the EOM through a 90/10 fiber beam splitter (the 10% of the light is used for monitor purpose). About 30mW light from the fiber laser is sent to the EOM. The EOM is mounted on a temperature-stabilized platform to maintain a stable and safe operation at 40.0 °C. To achieve high extinction ratios of modulation, two DC bias ports of the EOM are controlled by the YY Labs' dual-base-MZ modulator bias controller which stabilizes the EOM DC voltages using a feedback circuit based on the detected output power from the EOM. The EOM has a relatively high insertion loss (~6 dB). Under CW operation (no RF input), the maximum optical power from the EOM (measured after the beam splitter) is slightly over 6 dBm (4mW) when the EOM is manually biased at the peak. Using the bias controller to set the EOM bias at the null point, we are able to achieve the minimum output power from the EOM of −39 dBm (12.6nW), which results in a DC extinction ratio of 45 dB.

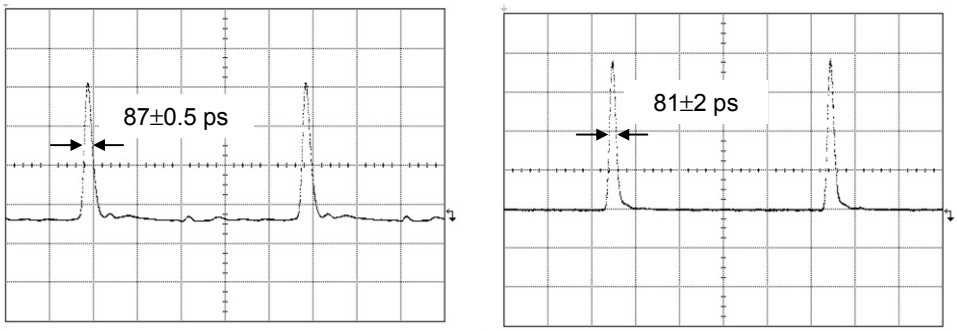

Fig. 3. (a) RF pulse waveform and (b) YDFA output optical pulse waveform. Time scale is 500 ps/div. The RF pulse generator design is AC coupled.

The high frequency pulse generator is customized by Picosecond Pulse Labs to produce ~80 ps/402.5 MHz RF pulses. To generate narrow optical pulses, the amplitude of the RF pulses is adjusted to be about 90% of the $V_{\pi/2}$ (~2 V) of the EOM modulator while the bias controller has been turned on to maintain a high DC extinction ratio. Under pulsed modulation, the peak optical power of the EOM output is found to be close to 4 mW. We have measured both the direct EOM output and its amplification (~30 dB gain) from the YDFA using a fast photodiode (New Focus 1444 with the rise time 18.5 ps) and an Agilent sampling oscilloscope. The pulse waveform of both the direct EOM output and the YDFA output have Gaussian-like profiles and both pulse widths are measured to be 81 ± 2 ps. Meanwhile, the RF modulation signal has a pulse width of 87 ± 0.5 ps. Figure 3 shows the waveforms of the RF pulses and YDFA output light pulses (at the peak output power of ~2.2 W). The optical pulse is narrower than the RF signal due to the small amplitude ($<V_{\pi/2}$) modulation. Considering the effects of photodiode response time and cable, we speculate that the actual laser pulse width is around 80 ps. We have also measured the noise floor level of the YDFA output and found it to be comparable to the noise floor level of the EOM output when there is no pulse modulation. The result indicates that a very high contrast of the optical pulses has been achieved with the bias control of EOM.

3.2 Output power

We have measured both the IR and UV light output powers of the laser as a function of the YDFA output power (average). The YDFA output power is varied up to 75 mW that is

#183038 - $15.00 USD Received 8 Jan 2013; revised 25 Mar 2013; accepted 28 Mar 2013; published 4 Apr 2013

limited by its amplification capacity. Two macropulse settings, 10-μs/10-Hz and 5-μs/10-Hz, have been tested in the experiment. For the 10-μs/10-Hz macropulse setting, we measured the maximum macropulse energy to be 26 mJ after the 6 mm amplifiers, 700 mJ after the 9 mm amplifiers, and 135 mJ after the third harmonic conversion. While for the 5-μs/10-Hz macropulse setting, the corresponding values are 13 mJ, 500 mJ, and 145 mJ, respectively. Higher conversion efficiency is achieved for the 5-μs setting due to the higher pulse energy of micropulses. Figure 4 shows the UV light macropulse energies as a function of the YDFA output power for both 10-μs and 5-μs macropulse settings. While the power saturation occurs for both settings, the 10-μs setting shows saturation at an earlier stage. The saturation is mainly due to that of the Nd:YAG amplifiers. We have also measured the ASE content of the laser output by applying the same pump power while turning off the seeder output. The IR output shows about 7% (0.5 W/7 W) of the ASE content while the UV light has only 0.25% (3 mW/1.35W) of the ASE content.

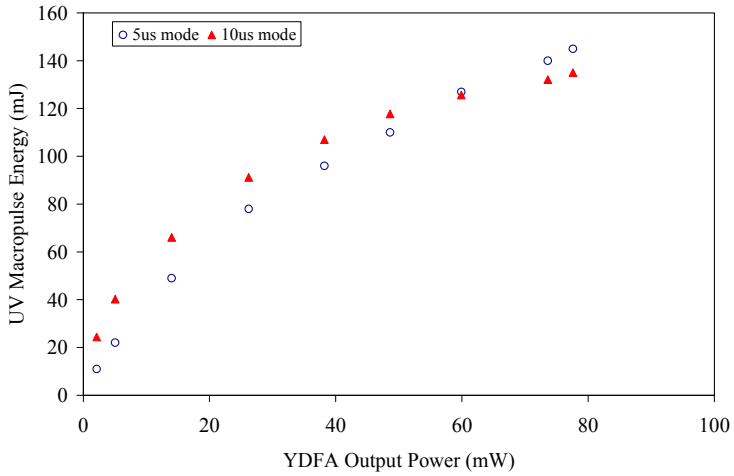

Fig. 4. Measured UV macropulse energies versus YDFA average output power.

3.3 Spatial profiles

Beam profiles of both IR and UV lights are measured using an externally triggered beam profiler (DataRay WinCamD). The IR beam right after the 9mm amplifiers is shown in Fig. 5(a). The beam shows a very symmetrical distribution with a 4-sigma beam size of about 2.2 mm. A nearly perfect Gaussian profile has been obtained for the UV beam as shown in Fig. 5(b). The profile also shows a symmetric distribution with the full-width-half-maximum (FWHM) angles of 0.23 × 0.22 $mrad^2$. The beam quality of the UV beam has been measured in the far-field and the M^2 number is estimated to be less than 1.1.

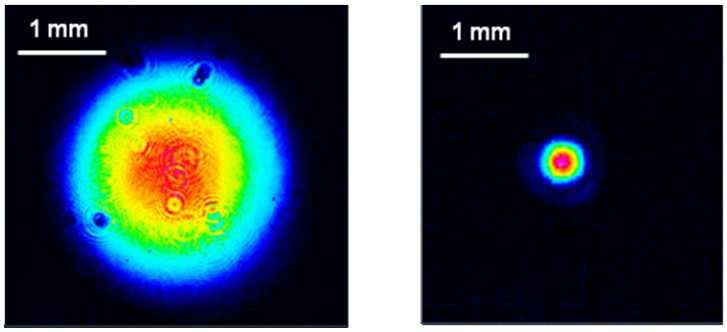

Fig. 5. IR and UV beam profiles.

#183038 - $15.00 USD Received 8 Jan 2013; revised 25 Mar 2013; accepted 28 Mar 2013; published 4 Apr 2013

3.4 Temporal waveforms

A typical 10-μs UV macropulse waveform is shown in Fig. 6. The macropulse shows a flat profile with the standard variation of < 5% of its amplitude. Similar uniform profiles have been obtained on 5-μs UV macropulses. The micropulse waveform of the UV beam cannot be directly measured due to the bandwidth limitation of the photo detector at the UV wavelength range. We have evaluated the UV micropulses using two different approaches. First, we conduct a direct measurement of the micropulse waveform of the IR beam using the fast photodiode and sampling oscilloscope. Figure 7 shows the measured waveforms of micropulse of the IR beam. The pulse width is measured to be 83 ps. The pulse width of the UV light is then estimated from that of the IR light by considering two mechanisms: the pulse narrowing in the harmonic/sum-frequency generations and the pulse broadening (temporal walk-off) due to the group velocity mismatch (GVM) in two crystals. Using the GVM = 44 fs/mm in the doubler and GVM = 280 fs/mm in the tripler provided from the vendor, we calculated the UV pulse width as $\tau_{UV} = \tau_{IR} / \sqrt{3} + \tau_{GVM} \approx 48\,\text{ps} + 10\,\text{ps} = 58\,\text{ps}$. Our second approach is to estimate the pulse widths of IR and UV micropulses through the optical correlation measurements. Both the auto-correlation between two IR beams and the cross-correlation between the IR and UV beams are measured using a LBO type II crystal in a non-collinear configuration. Based on the correlation measurement results, we estimate the pulse width of the IR beam to be about 85 ps and that of the UV pulse to be 66 ps. While the IR pulse width is close to that in the first measurement, the UV pulse width is 15% larger than that in the first measurement. We consider the discrepancy is due to walk-off of the beams and possible correlation measurement error caused by the thickness of the LBO crystal. Further measurements will be conducted to improve accuracy. Using the 66-ps pulse width, we estimate that the maximum peak power of the UV micropulses is 0.5 MW with the 10-μs/10-Hz macropulse setting and 1.08 MW with the 5-μs/10-Hz setting.

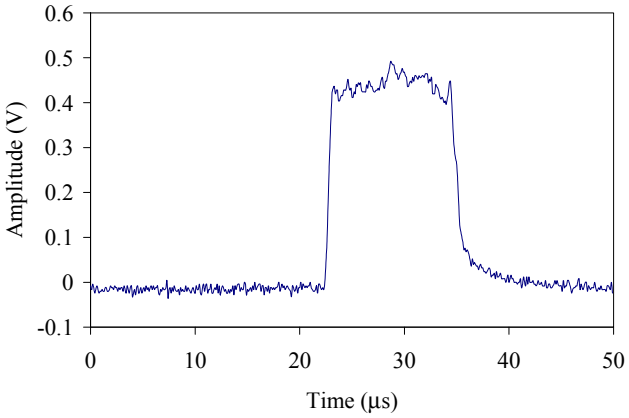

Fig. 6. Macropulse of the UV light beam.

#183038 - $15.00 USD Received 8 Jan 2013; revised 25 Mar 2013; accepted 28 Mar 2013; published 4 Apr 2013

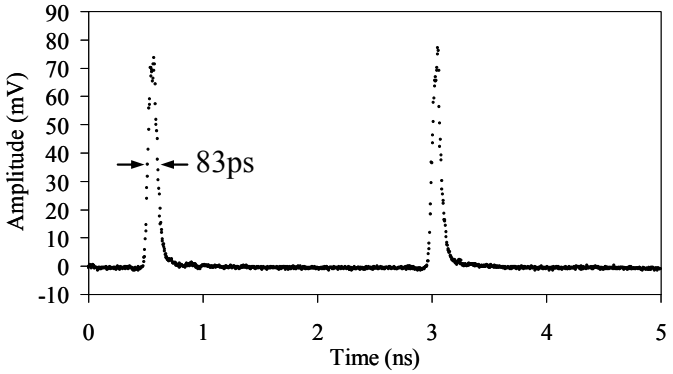

Fig. 7. Micropulse waveforms of the IR light beam.

3.5 Spectrum

The optical spectrum and the linewidth of individual mode are key factors for our application which uses a coherent light to excite hydrogen atoms at high energies. In particular, our seeder laser is constructed through a direct picosecond pulse modulation of a single frequency light, it is important to verify how the spectrum of the light changes after the modulation. The optical spectrum of the laser is measured by a heterodyne beating of the YDFA output with a reference beam that is taken from the same fiber laser source in Fig. 1 with a 40-MHz frequency offset. The reconstructed optical spectrum is shown in Fig. 8. The FWHM of the spectrum is estimated to be 5.5 GHz. The time-bandwidth product is about 0.45 which indicates the generated pulses are transform-limited.

The timing jitter of the laser pulse is measured using a power spectral density technique [15] that utilizes high harmonics of the fundamental signal to separate out the timing (phase) noise from the amplitude noise. We used "Phase Noise" function of the spectrum analyzer (Agilent E4440A) and chose the carrier frequency at 805 MHz (2nd harmonic of the repetition rate) and the integration range over 10 Hz - 10 kHz. The jitter is measured to be 2.2 ps that is mainly caused by the modulation RF signal of the EOM. The timing jitter of the RF signal is measured to be 2.16 ps.

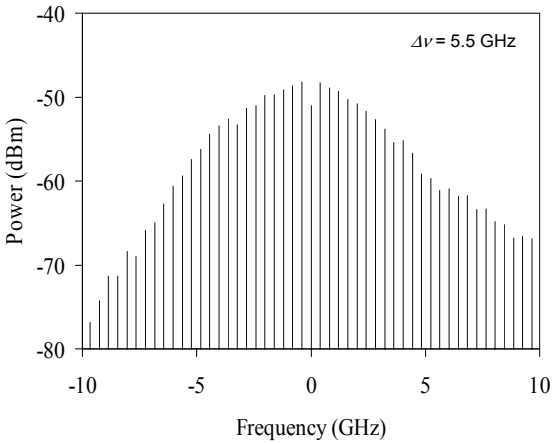

Fig. 8. Measured optical spectrum of the IR light via wave mixing. The FWHM is about 5.5 GHz. Mode spacing is 402.5 MHz.

#183038 - $15.00 USD Received 8 Jan 2013; revised 25 Mar 2013; accepted 28 Mar 2013; published 4 Apr 2013

The linewidth of individual longitudinal modes in Fig. 8 have been investigated using both a delayed self-heterodyne interferometer (DSHI) [16] and a scanning Fabry-Perot resonator with a full spectrum range of 402.5 MHz. The resolution of the DSHI is of the order of 100 KHz while that of the Fabry-Perot resonator is of the order of 1 MHz. In both cases, we were unable to resolve the linewidth under the above limitation. Using the theoretical model derived in Ref [17], we calculated that the linewidth of individual laser modes are close to that of the fiber laser. A precise measurement will be conducted in the future using a different heterodyne measurement approach [18] which involves a second frequency stable tunable laser source.

4. Conclusion

In summary, we have described a MOPA configuration macropulse laser system that provides MW peak power at 355 nm. The seed laser is based on a direct modulation of a single frequency light from a fiber laser with 5 KHz linewidth. Using an adaptive bias control, the seed laser is capable of generating transform-limited picosecond pulses with high contrast ratio, flexible pulse width, and small timing jitter. The Continuum customized multi-stage burst mode laser amplifier enables high gain, effective ASE suppression, and uniform macropulse shaping with tunable macropulse durations and repetition rates. The laser demonstrated 66-ps/402.5-MHz output pulses with 1.08 MW peak power at 355 nm for the 5-μs/10-Hz macropulse setting. The laser output has a very stable spectrum with the individual mode linewidth below 100 KHz. The mode-hopping free narrow linewidth light is critical for the beam recycling optical cavity designed for mitigation of the average laser power requirement [19]. Although the laser parameters are optimized for the application of laser-assisted H^- beam stripping at the Spallation Neutron Source, the designed system has a broad flexibility in terms of pulse width and repetition rate (of both macropulses and micropulses) and therefore can be used in many other applications.

Acknowledgments

The authors acknowledge Dr. J. Zhu from Continuum for his development and technical support of the customized amplifier system and Dr. M. Notcutt from Boulder Precision Electro-Optics for helpful discussions on the seeder development. Support and technical helps from ORNL members A. Aleksandrov, A. Webster, J. Diamond are acknowledged. ORNL is managed by UT-Battelle, LLC, under contract DE-AC05-00OR22725 for the U.S. Department of Energy. This work was performed under the auspices of the Department of Energy, Office of Science/Basic Energy Sciences.

#183038 - $15.00 USD Received 8 Jan 2013; revised 25 Mar 2013; accepted 28 Mar 2013; published 4 Apr 2013